

# Multiscale modeling of the anisotropic shock response of $\beta$ -HMX molecular polycrystals

Amir R. Zamiri\* and Suvranu De

*Mechanical, Aerospace and Nuclear Engineering Department, Rensselaer Polytechnic Institute,  
110 8<sup>th</sup> St. Troy, NY 12180, USA*

*(Received November 11, 2010, Accepted February 18, 2011)*

**Abstract.** In this paper we develop a fully anisotropic pressure and temperature dependent model to investigate the effect of the microstructure on the shock response of  $\beta$ -HMX molecular single and polycrystals. This micromechanics-based model can account for crystal orientation as well as crystallographic twinning and slip during deformation and has been calibrated using existing gas gun data. We observe that due to the high degree of anisotropy of these polycrystals, certain orientations are more favorable for plastic deformation – and therefore defect and dislocation generation – than others. Loading along these directions results in highly localized deformation and temperature fields. This observation confirms that most of the temperature rise during high rates of loading is due to plastic deformation or dislocation pile up at microscale and not due to volumetric changes.

**Keywords:** high rate of loading; shock; multiscale modeling; energetic crystals;  $\beta$ -HMX.

---

## 1. Introduction

While significant advances have been made in understanding the chemistry of detonation processes of polymer-bonded explosive (PBX) materials, the modeling of the thermo-mechanics of such materials has been thwarted by a lack of appropriate computational tools which link disparate length scales from the microstructural level to the system level. PBXs are composed of a very high volume fraction of explosive crystals with a wide range of sizes bonded together by a rather weak polymer matrix (Baer *et al.* 2007). It is well known that the heterogeneity of the microstructure has a profound effect on the bulk material response of PBXs. Hot spots result from energy accumulation in localized regions raising the local temperature of the explosive to the ignition point (Dick *et al.* 2004).

Microstructural damage is known to facilitate detonation at relatively low velocity impacts. Hence continuum mechanics-based techniques such as Lagrangian finite element methods or Eulerian hydrocodes which use constitutive relations that do not account for the microstructure have questionable reliability beyond their range of calibration. Molecular dynamic (MD) and *ab initio* quantum mechanical models are excellent for predicting reaction rates and mechanisms using small sample sizes but are computationally expensive and, even with the current advances in computational

---

\* Corresponding author, Ph.D., E-mail: [zamira@rpi.edu](mailto:zamira@rpi.edu), [amir.zamiry@gmail.com](mailto:amir.zamiry@gmail.com)

power, it is not possible to predict the mechanical response of systems of practical size in realistic time. For example, state-of-the-art MD simulations are restricted to about  $10^9$  atoms for a few nanoseconds and computational quantum mechanical tools are restricted to a much smaller system of about 100-1000 atoms.

Previous investigations have shown that molecular crystals such as energetic molecular crystals are rather brittle with a low range of plastic deformations (Hooks *et al.* 2006). However, the small amount of plastic deformation may significantly affect material response. For example, in energetic materials, the anisotropic plastic behavior and the amount of plastic deformation in the molecular crystalline part of the microstructure have significant effects on the performance of heterogeneous explosive materials and solid propellants (Bowden *et al.* 1952). It has been observed that in energetic molecular crystals, plastic flow permanently deforms and distorts both lattice and molecular structure at all levels of deformation. The deformation is often localized in shear bands within the crystal at higher rates of deformation. These pile up of defects and dislocations may lead to a localized temperature increase which itself may generate hot spots necessary for detonation in such materials (Walley *et al.* 2006).

In previous works, the crystalline part of the microstructure has been modeled using relatively simple phenomenological equations (Baer *et al.* 2007). However, the plastic yielding in energetic crystals such as  $\beta$ -HMX is highly anisotropic and orientation dependent and use of such phenomenological constitutive equations is not adequate. A model based on anisotropic crystal plasticity also has been developed to model shock response of  $\beta$ -HMX (Barton *et al.* 2009). Although this model accounts for anisotropy, several assumptions have been made to simplify the thermomechanics of the model.

To alleviate these problems multiscale computational tools that link various length and time scales are necessary. Such techniques allow the prediction of bulk material response based on microstructural information (Zhang *et al.* 2008, Matou and Maniatty 2009). Previously developed multiscale methods either assume linear elastic properties of the binder and particles (Macri *et al.* 2006) or simplified phenomenological models (Baer *et al.* 2007). However, experimental evidence indicates that nonlinear constitutive properties of the polymer binder, anisotropic plasticity of the energetic crystals together with decohesion of the particle-matrix interface must be considered for accurate prediction of hotspot formation (Macri *et al.* 2006, Rae *et al.* 2006).

As a first step towards achieving this goal, in section 2 of this paper we focus on development of an efficient pressure and temperature dependent micromechanical model based on a single crystal yield function to predict the complex anisotropic elastoplastic response of energetic molecular crystals of  $\beta$ -HMX under shock loading. This model can account for crystal orientation as well as crystallographic twinning and slip during deformation. A crystal hardening model is used to take into account the effects of temperature and pressure on the critical resolved shear stress of different slip and twin systems. In our formulation the pressure-volume-energy relation, known as the equation of state (EOS), is coupled with the crystal level model to account for pressure and volume changes at high rates of loadings. The model is calibrated using existing gas gun shot experimental data for  $\beta$ -HMX. It is then used to simulate the shock and impact response of  $\beta$ -HMX single crystals along different crystallographic directions. In the next step, a multiscale approach is used in section 3 to model the effect of the microstructure on the overall performance of the polycrystalline HMX under high loading rate. Choice of material properties is in section 4 followed by some numerical results in section 5. Although our focus is on  $\beta$ -HMX in this paper, this model can be applied to other energetic molecular crystals.

## 2. A micromechanical model of $\beta$ -HMX single crystals

Octahydro-1,3,5,7-tetranitro-1,3,5,7-tetrazocine (HMX) is a molecular polycrystal which is extensively used as explosives and rocket propellants. HMX exhibits three pure crystal polymorphs at ambient pressure, which can be ranked in terms of their stability with increasing temperature as  $\beta$ -,  $\alpha$ -, and  $\gamma$ -HMX (Palmer *et al.* 1982). The most stable polymorph of HMX is  $\beta$ -HMX at room temperature and pressure. The crystal structure of  $\beta$ -phases of HMX is monoclinic ( $P2_1/c$  or, equivalently,  $P2_1/n$  space group,  $Z=2$  molecules per unit cell, symmetry axis =  $b$ ; 13 independent elastic coefficients). The crystallographic constants for the unit cell of this primitive monoclinic structure are 0.654 nm, 1.105 nm, and 0.736 nm for  $a$ ,  $b$ , and  $c$ , respectively with the monoclinic angle of  $102.66^\circ$ .

At high rates of loading the deformation is a function of the temperature ( $T$ ) and pressure ( $P$ ). The deviatoric ( $\hat{\sigma}'$ ) and volumetric ( $\hat{\sigma}_h$ ) components of the stress ( $\hat{\sigma}$ ) in the deformed but unrotated crystal coordinate may be represented by

$$\hat{\sigma}' = \ell : \mathbf{C} : \boldsymbol{\varepsilon}'^e + \frac{1}{3} (\ell : \mathbf{C} : \mathbf{I}) \boldsymbol{\varepsilon}_v^e + \rho \Gamma' T \Delta S \quad (1)$$

$$\begin{aligned} \hat{\sigma}_h = P_{EOS} + \frac{1}{3} (\boldsymbol{\varepsilon}'^e : \mathbf{C} : \mathbf{I}) - \rho \Gamma_m T \Delta S + \left[ \frac{1}{2} \left( \boldsymbol{\varepsilon}'^e : \frac{d\mathbf{C}}{dP} : \boldsymbol{\varepsilon}'^e \right) + \frac{1}{3} \left( \boldsymbol{\varepsilon}'^e : \frac{d\mathbf{C}}{dP} : \mathbf{I} \boldsymbol{\varepsilon}_v^e \right) \right] \frac{dP}{d\boldsymbol{\varepsilon}_v^e} \\ + \left[ \frac{1}{2} \left( \boldsymbol{\varepsilon}'^e : \frac{d\mathbf{C}}{dT} : \boldsymbol{\varepsilon}'^e \right) + \frac{1}{3} \left( \boldsymbol{\varepsilon}'^e : \frac{d\mathbf{C}}{dT} : \mathbf{I} \boldsymbol{\varepsilon}_v^e \right) \right] \frac{dT}{d\boldsymbol{\varepsilon}_v^e} \end{aligned} \quad (2)$$

where  $P_{EOS}$  is pressure given by the equation of state (see section 2.3 below),  $\Gamma'$  is the deviatoric part of the Grüneisen tensor,  $\Delta S$  is the change in entropy,  $\mathbf{C}$  is the elastic tensor,  $\boldsymbol{\varepsilon}'^e$  the deviatoric elastic part of the logarithmic strain tensor,  $\boldsymbol{\varepsilon}_v^e = \boldsymbol{\varepsilon}^e : \mathbf{I}$  is the volumetric part of the strain, and  $\ell$  is a fourth rank tensor defined as  $\ell = \ell' - \frac{1}{3} \mathbf{I} \otimes \mathbf{I}$ .

Previous investigations have shown both slip and twin are responsible for plastic deformation of  $\beta$ -HMX (Dick *et al.* 2004, Palmer *et al.* 1982). To model this type of deformation, let us consider an orthogonal coordinate system for a unit cell of  $\beta$ -HMX crystal as shown in Fig. 1. Any slip/twin system ( $\alpha$ ) in the crystal can be defined by a unit vector normal to the slip plane ( $\mathbf{m}^\alpha$ ) and a unit vector along the slip direction ( $\mathbf{s}^\alpha$ ). The resolved shear stress on slip system is

$$\tau^\alpha = \boldsymbol{\sigma} : \mathbf{P}^\alpha \quad (3)$$

where  $\boldsymbol{\sigma}$  is the Cauchy stress tensor and  $\mathbf{P}^\alpha$  is a matrix defining the orientation of the slip system  $\alpha$  with respect to the crystal coordinate system ( $a'b'c'$ )

$$\mathbf{P}^\alpha = \frac{1}{2} [\mathbf{m}^\alpha \otimes \mathbf{s}^\alpha + (\mathbf{m}^\alpha \otimes \mathbf{s}^\alpha)^T] \quad (4)$$

We define the following yield function for any slip system  $\alpha$

$$f_\alpha(\boldsymbol{\sigma}, \mathbf{q}) = \frac{|\tau^\alpha|}{\tau_y^\alpha} - 1 \quad (5)$$

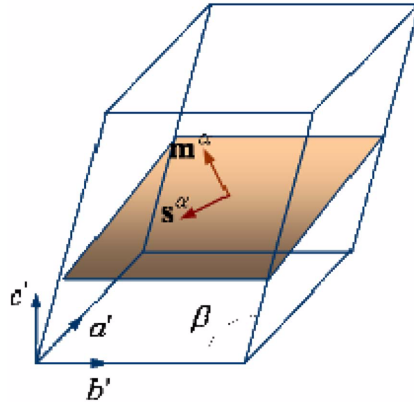


Fig. 1 A monoclinic crystal structure with a slip/twin system

where  $\tau_y^\alpha$  is the critical shear stress on the slip plane. The number of yield functions in a crystal depends on the number of slip/twin systems present in the crystal. To describe the overall yield criterion for a single crystal, we define the following “combined constraints yield function” (Zamiri and Pourboghrat 2010)

$$f(\sigma, \tau_y^\alpha) = \frac{1}{\kappa} \ln \left\{ \sum_{\alpha=1}^N \exp \left[ \frac{\kappa}{m} \left( \frac{|\tau^\alpha|}{\tau_y^\alpha} - 1 \right) \right] \right\} \quad (6)$$

where  $m$  and  $\kappa$  are material parameters which control the shape of the single crystal yield surface. For most materials  $m = 1$  and  $\kappa$  is obtained using the stacking fault energy of the material or experimental data. A value of  $\kappa = 80$  was used for  $\beta$ -HMX (Zamiri and De 2010).  $N$  is the total number of slip/twin systems in the crystal.

### 2.1 Hardening model

We assume that the critical resolved shear stress ( $\tau_y^\alpha$ ) for both slip and twin can be modeled as the following rate sensitive power law hardening form as (Becker 2004)

$$\tau_y^\alpha = \frac{\mu}{\mu_0} \tau_0 [1 + B(\bar{\gamma} + \gamma_0)^n] \left( \frac{|\dot{\gamma}^\alpha| + \dot{\gamma}_{off}}{\dot{\gamma}_0} \right)^m \exp(-\lambda T \Delta S) \text{sgn}(\dot{\gamma}^\alpha) \quad (7)$$

where  $\mu$  is the elastic shear modulus,  $\gamma_0$ ,  $\dot{\gamma}_{off}$ ,  $\dot{\gamma}_0$  and  $\lambda$  are materials parameters,  $\tau_0$  is initial critical resolved shear stress, and  $\bar{\gamma}$  is the total accumulated shear strain on all slip systems

$$\bar{\gamma} = \sum_{\alpha=1}^N \int_0^t |\dot{\gamma}^\alpha| dt \quad (8)$$

### 2.2 Temperature

At high rates of deformation, the temperature of the material changes due to both volume change and plastic deformation. The temperature can be expressed as (Menikoff *et al.* 2002)

$$T(V, e) = T_0 \left( \frac{V_0}{V} \right)^\Gamma + \frac{e - e_s(V)}{C_v} \quad (9)$$

where  $e$  is the specific internal energy, the index  $s$  denotes the initial value,  $C_v$  is the specific heat at constant volume, and  $V$  is the specific volume ( $\text{cm}^3/\text{gr}$ ).

The first term in Eq. (9) is related to the volume change and the second term denotes the dissipative heat which is mostly due to the plastic deformation. Here we assume that the change in the internal energy is equal to the plastic work.

### 2.3 Equation of state

An equation of state (EOS) is used to compute pressure due to pure volume change in the material. For  $\beta$ -HMX, we use the EOS proposed by Yoo and Cynn [Yoo *et al.* 1999] by fitting their data to a third-order Birch-Murnaghan equation of state

$$P_{EOS}(V) = \frac{3}{2} K_{T_0} \left[ (V_0/V)^{\frac{7}{3}} - (V_0/V)^{\frac{5}{3}} \right] \left[ 1 + \frac{3}{4} (K'_{T_0} - 4) \left[ (V_0/V)^{\frac{2}{3}} - 1 \right] \right] \quad (10)$$

where  $K_{T_0}$  and  $K'_{T_0}$  are bulk modulus and the derivative of the bulk modulus at initial temperature  $T_0$ , respectively.

## 3. Multiscale modeling of polycrystalline $\beta$ -HMX

Unlike linear analysis, in nonlinear multiscale modeling the constitutive behavior at the macroscale may not be assumed *a priori*. Some of the existing multiscale strategies that are applicable to nonlinear analysis either assume *a priori* macroscale material models or perform ad hoc macro-micro couplings (Mang *et al.* 2009). Most of such multiscale techniques are computationally very expensive, especially for materials with complex microstructures like particulate composites (for more information see Matou and Maniatty 2009, Wang and Fang 2010, Kaczmarek 2010) Hence, in this paper we have used a Taylor type homogenization approach which has been successfully applied to other polycrystalline systems (Taylor 1983).

The key feature of this strategy is that no constitutive assumptions are made at the macroscale and the stress-strain relationship is developed at each integration point on the fly. In a previous work we have demonstrated that the yield function of  $\beta$ -HMX is highly anisotropic and it is not possible to develop a closed-form constitutive model (Zamiri and De 2010). The material is highly elastic along certain orientations, while along others it is elasto-plastic. Hence, it is necessary to use an equation-free multiscale strategy.

In our multiscale approach we consider three scales (Fig. 2): a *microscopic* scale that represents single crystals of the energetic materials at length scales of the order of nm- $\mu\text{m}$ , a *meso-scale* which represents the polycrystal ( $\mu\text{m}$ -mm) and the *continuum* level (mm) which represents the macroscopic sample under loading. The overall response of the polycrystal is then simulated within the multiscale framework for complex nonlinear loading paths including shock response.

In the Taylor type homogenization approach, each grain of the polycrystal aggregate undergoes homogeneous deformation and deformation rate. Therefore, the velocity gradients in all grains are

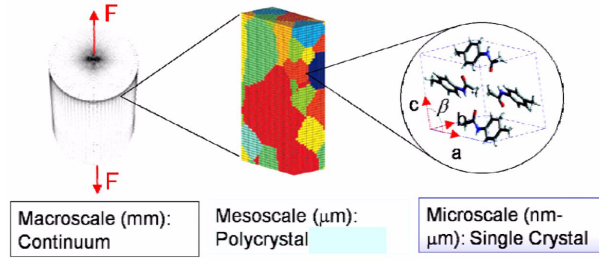


Fig. 2 Scales that are coupled through the multiscale approach

the same and equal to the overall velocity gradient. The velocity gradient ( $\mathbf{L}$ ) in the material coordinate system can be decomposed into a rate of deformation ( $\mathbf{D}$ ) and a spin tensor ( $\mathbf{W}$ ) as

$$\mathbf{L} = \mathbf{D} + \mathbf{W} \quad (11)$$

According to the Taylor model,  $\mathbf{W}$  would have to be the same for all grains and equal to the global  $\mathbf{W}$ . However, it must be mentioned that the elastic part of the spin ( $\mathbf{W}^e$ ) and the plastic part ( $\mathbf{W}^p$ ) are different for different grains.

The volume average of a local tensorial quantity  $\mathbf{t}(\mathbf{x})$  is defined as

$$\langle \mathbf{t} \rangle = \frac{1}{V} \int_V \mathbf{t}(\mathbf{x}) dV \quad (12)$$

The macro-scale stress tensor in a polycrystalline material may be expressed as

$$\langle \boldsymbol{\sigma} \rangle = \frac{1}{V} \int_V \boldsymbol{\sigma}^c(\mathbf{x}) dV \quad (13)$$

where  $\boldsymbol{\sigma}^c(\mathbf{x})$  is the stress in the grain 'c'. Assuming that  $\boldsymbol{\sigma}^c(\mathbf{x})$  is constant over the grain and all grains have the same volume ( $V^c$ ), Eq. (13) can be rewritten as

$$\langle \boldsymbol{\sigma} \rangle = \frac{V^c}{V} \sum_c \boldsymbol{\sigma}^c = \frac{1}{M} \sum_c \boldsymbol{\sigma}^c \quad (14)$$

where  $M$  is the number of grains. Eq. (14) is then used in an explicit algorithm to calculate the macro stress tensor from the crystal stress tensors.

#### 4. Materials parameter estimation for $\beta$ -HMX

Table 1 presents all the 13 elastic constants that we have used for  $\beta$ -HMX (Sewell *et al.* 2003). Since the pressure and temperature dependent elastic constants for  $\beta$ -HMX are not available, we treat them to remain constants in our entire simulations. The other parameters needed for the multiscale simulations are:  $K_{T_0} = 12.4 \text{ GPa}$ ,  $K'_{T_0} = 10.2$ ,  $C_v = 1.5 \times 10^{-3} (\text{MJ/kg})/K$ ,  $\Gamma = 1.1$ , and  $\rho_0 = 1.9 \text{ g/cm}^3$  (Menikoff *et al.* 2002).

The hardening parameters were found by calibrating against gas gun data performed on single crystals of HMX along [110] and [011] crystallographic directions (Dick *et al.* 2004). The hardening parameters were found to be;  $B = 4.5$ ,  $n = 0.2$ ,  $m = 0.01$ ,  $\gamma_0 = 0.0$ ,  $\dot{\gamma}_{off} = 85 \times 10^{-8}$ ,  $\dot{\gamma}_0 = 4.0 \times 10^{-3}$ ,  $\lambda = -5.15 \times 10^{-4}$ ,  $\tau_0 = 103 \text{ MPa}$ .

Table1 Elastic constants for  $\beta$ -HMX (GPa)

$C_{11}$	$C_{12}$	$C_{13}$	$C_{15}$	$C_{22}$	$C_{23}$	$C_{25}$	$C_{33}$	$C_{35}$	$C_{44}$	$C_{46}$	$C_{55}$	$C_{66}$
22.2	19.6	213.2	-0.1	23.9	13.0	4.7	23.4	1.6	9.2	2.5	11.1	10.1

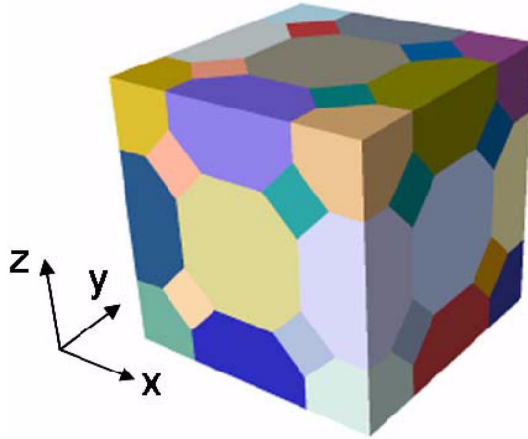


Fig. 3 the polycrystalline unit cell used in these simulations. The size of the unit cell is  $40\ \mu\text{m} \times 40\ \mu\text{m} \times 40\ \mu\text{m}$  and contains 35 grains

## 5. Simulation results

### 5.1 Computational models

The model presented in the previous section was implemented into Abaqus finite element code (Simulia, Providence, RI) as VUMAT and used to simulate the shock response of  $\beta$ -HMX single crystals along different crystallographic directions as well as a polycrystalline configuration. The single crystal model of dimension  $10\text{mm} \times 10\text{mm} \times 10\text{mm}$  was discretized using 8000 brick elements and loaded along the [110] and [010] crystallographic directions. The four faces of the model normal to loading direction were constrained. A time varying pressure load was ramped from zero to 2 GPa in  $0.01\ \mu\text{s}$  and applied to one of the faces normal to the  $x$ -direction while the opposite face was maintained traction-free.

To further investigate the effects of the crystal misorientation on the shock response and temperature distribution, a polycrystalline unit cell ( $40\ \mu\text{m} \times 40\ \mu\text{m} \times 40\ \mu\text{m}$ ) composed of 35 grains was developed (Fig. 3). The boundary conditions were the same as mentioned above except for the pressure which was ramped up to 2GPa in 0.01 ns.

Fig. 4 shows the yield function corresponding to the different crystallographic orientations clearly underscoring the anisotropic nature of the plastic response. Fig. 5 shows the dynamic response of a  $\beta$ -HMX single crystal. The shock response is quite different along the [110] and [010] crystallographic directions. The same behavior has been observed in gas gun experiments on  $\beta$ -HMX (Dick *et al.* 2004). Based on such experiments, loading along [010] direction does not lead to a significant plastic deformation in the crystal while much more plastic deformation is observed for loading along [110] direction of the crystal. The slip and twin systems can not get activated easily

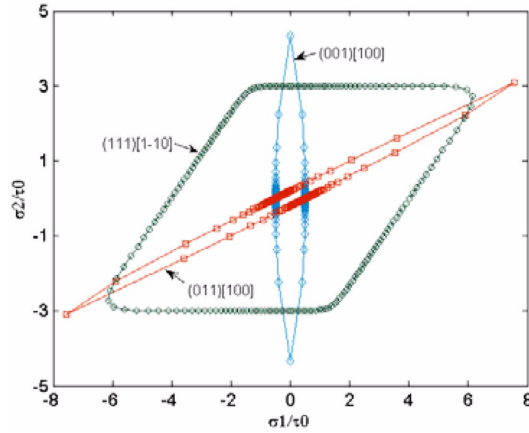


Fig. 4 The yield surfaces for 3 different orientations of (001)[100], (011)[100], and (111)[ $\bar{1}0$ ] in  $\beta$ -HMX single crystal

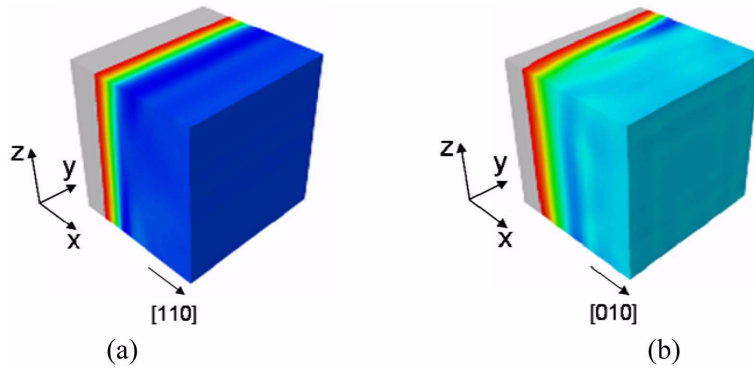
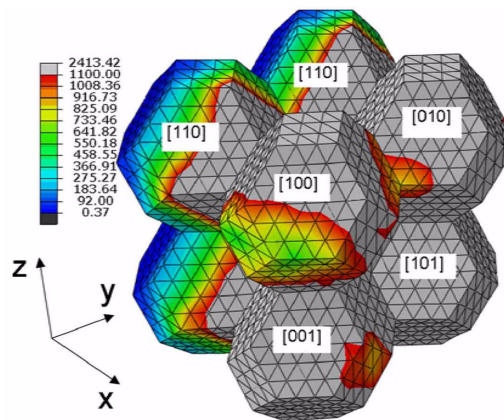


Fig. 5 The normal stress ( $\sigma_{xx}$ ) in a  $\beta$ -HMX single crystal for loading along: (a) [010] and (b) [110] directions at  $2.5 \times 10^{-6}$  s

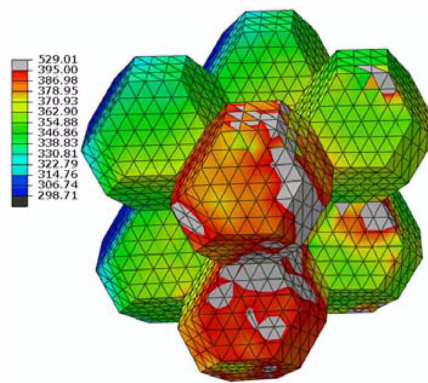
for the crystal loaded along [010] crystallographic direction. Such anisotropic elastic-plastic deformation behavior is responsible for anisotropic shock response of  $\beta$ -HMX molecular crystals.

Based on previous analysis (Zamiri and De 2010), for our polycrystalline model (Fig. 3), we choose the orientation of the grains in the interior of the model in such a way that some grains have a high propensity for plastic deformation while others remain more elastic. Fig. 6(a) shows the contour of the Mises stress after shock loading of the polycrystalline unit cell. The response is anisotropic which is due to the presence of the different orientations. Fig. 6(b) shows the temperature distribution which is also completely anisotropic. The temperature increase is rather high in most parts of the crystals with [100] and [001] orientations along the loading direction. These orientations are very soft and show significant plastic deformation at high rates of loading. Fig. 6(c) shows the distribution of the total accumulated slip  $\bar{\gamma}$ , which is a measure of the plastic deformation and dislocation density, in all grains. Crystals with [100] and [001] orientations (having their  $a$  or  $c$  crystal axis along the loading direction) exhibit highest plastic deformations which explains the higher temperature in these grains.

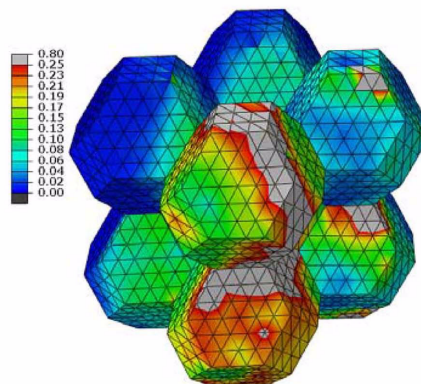
Grains with their [010] orientation with respect to the loading direction have been reported to



(a)



(b)



(c)

Fig. 6 The results of the simulation of shock loading on  $\beta$ -HMX microstructure: (a) misfit stress (MPa), (b) temperature (K) distribution and (c) distribution of accumulated slip after the shock has passed through the grains

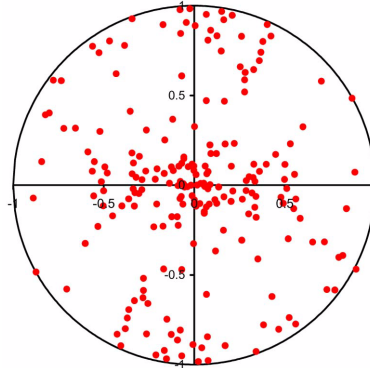


Fig. 7 (001) polefigure of  $\beta$ -HMX polycrystal used in these simulations

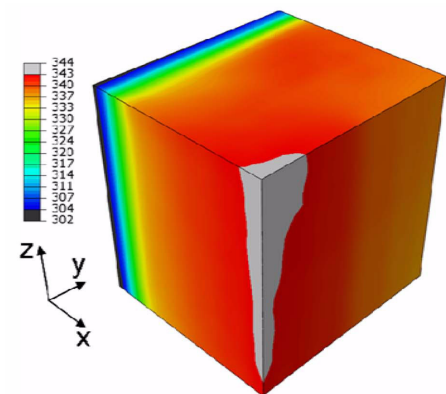
remain mostly elastic during the deformation (Dick *et al.* 2004, Zamiri and De 2010). Therefore, the temperature rise in these grains is mostly due to the pure pressure induced volume changes. Previous experiments have appeared that the temperature increase due to volume change can hardly go beyond 100K while a temperature increase of at least 200K is necessary for detonation initiation in  $\beta$ -HMX polycrystals (Menikoff *et al.* 2002). Our simulations show that this increase in temperature can be obtained through plastic deformation in the grains with soft orientations.

Further study of the Fig. 6(b) shows that although both [101] and [010] are almost hard orientations but due to the misorientation of these grains with the adjacent grains a localized plastic deformation might occur in some small regions of the grain which might lead to a local temperature increase in these grains.

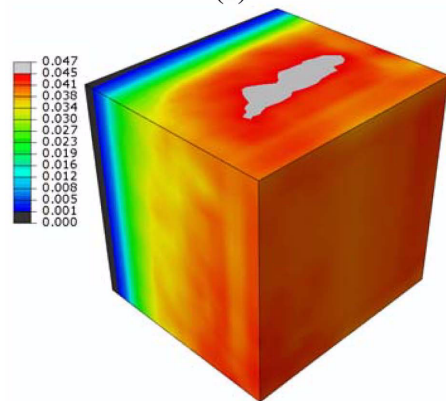
## 5.2 Multiscale polycrystalline model

The multiscale model presented in the previous section was used to simulate the shock response of  $\beta$ -HMX polycrystals with different textures. A computational model with dimension of  $10\text{mm} \times 10\text{mm} \times 10\text{mm}$  was discretized using 8000 brick elements and loaded along the  $X$ -axis at high rates of loadings. The four faces of the model normal to loading direction were constrained. A time varying pressure load was ramped from zero to 2 GPa in  $0.01 \mu\text{s}$  and applied to one of the faces normal to the  $X$ -direction while the opposite face was maintained traction-free. In the first set of simulations, at any integration point of the model, we used a texture which consisted of random orientations in terms of propensity for plastic and elastic deformations with respect to the loading direction. Fig. 7 shows the (001) polefigure for such texture. We considered the following three simulation scenarios with textures chosen based on the so-called “deformation distribution maps” of  $\beta$ -HMX presented in (Zamiri and De 2010):

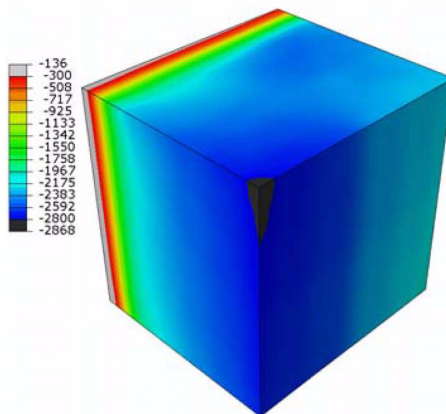
- Case 1:** A texture with 100 **randomly oriented grains** was considered at each macroscale integration point.
- Case 2:** A texture with 5 grains with **highly plastic** orientations of (001)[100], (010)[100], (010)[101], (010)[001], and (110)[001] were assumed at each integration point with their  $[uvw]$  directions along the loading direction ( $X$ -axis).
- Case 3:** A texture with 5 grains with **low plastic** orientations of (001)[010], (001)[0 $\bar{1}$ 0],



(a)



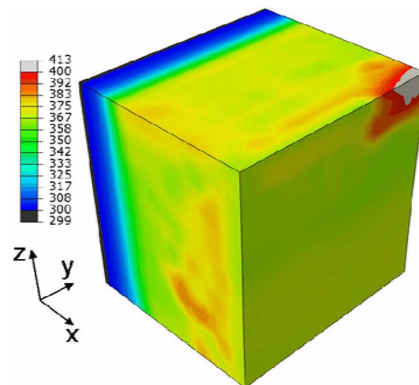
(b)



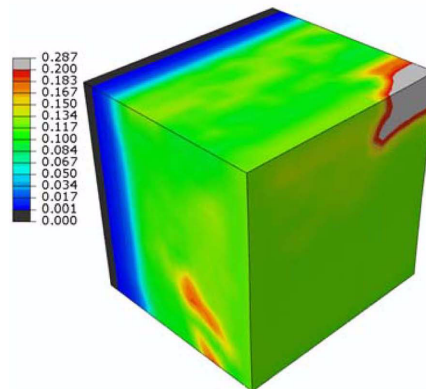
(c)

Fig. 8 Simulation results for the case having 100 random texture at each integration point: (a) temperature distribution ( $K$ ), (b) average accumulated slip ( $\bar{\gamma}$ ), and (c) pressure distribution (MPa)

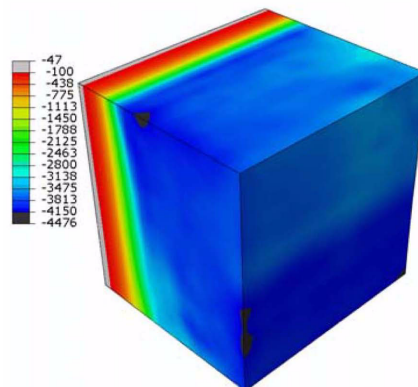
$(101)[010]$ ,  $(011)[2\bar{1}1]$ , and  $(00\bar{1})[010]$  were assumed at each integration point with their  $[uvw]$  directions along the loading direction ( $X$ -axis).



(a) Temperature distribution (K)



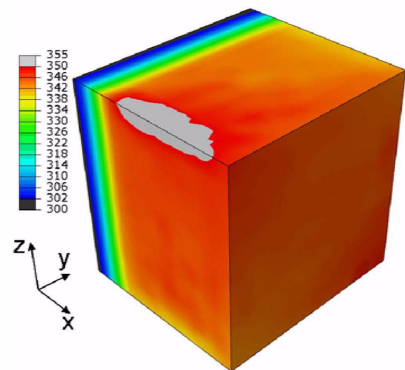
(b) Average accumulated slip



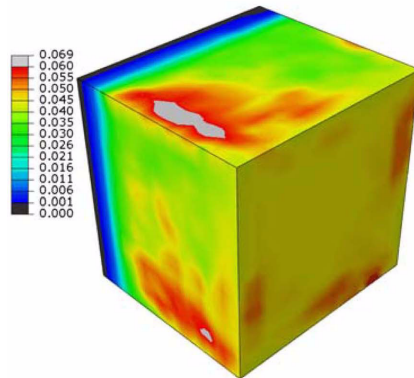
(c) Pressure distribution (MPa)

Fig. 9 Results of multiscale simulation for case 2 in which there is a texture with 5 grains with highly plastic orientations at each integration point: (a) temperature distribution (K), (b) average accumulated slip ( $\bar{\gamma}$ ), and (c) pressure distribution (MPa)

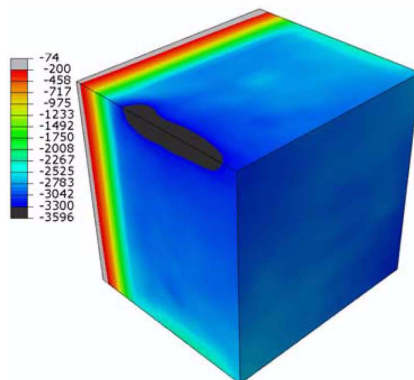
Fig. 8(a) shows the results of the temperature distribution Case 1. There is only 50K increase in temperature with no localization. Fig. 8(b) shows the accumulated slip which is a measure of the



(a) Temperature distribution (K)



(b) Average accumulated slip



(c) Pressure distribution (MPa)

Fig. 10 Results of multiscale simulation for case 3 in which at each integration point there are 5 grains with low plastic deformation propensity: (a) temperature distribution (K), (b) average accumulated slip ( $\bar{\gamma}$ ), and (c) pressure distribution (MPa)

dislocations density and plastic deformation. As can be seen the accumulated slip is very small in this case. Fig. 8(c) shows the hydrostatic pressure distribution. The temperature is maximum where the hydrostatic pressure is maximum. Since the temperature rise at high rate of loading is related to

both the plastic work and volume change, most of the temperature increase in this case is due to the volume change.

Fig. 9 shows the results for Case 2. Fig. 9(a) shows a large localized temperature raise. Fig. 9(b) and 9(c) show the accumulated slip and hydrostatic pressure distributions. The accumulated slip is much higher compared to the case 1 and is more intense in the region with high temperature raise. The pressure is also maximum in this region.

Finally, the simulation results for case 3 are presented in Fig. 10. It is observed that the plastic work is very small and therefore, most of the temperature rise is due to the volume change which is not very high.

From these three cases, it may be concluded that plastic deformation, and not volume change, is the major determinant of the very high local temperature increase during high rates of loading.

## 6. Conclusions

We have developed a thermo-micromechanical model to predict the effect of the micro structure on overall shock response and local temperature rise in  $\beta$ -HMX. This is, of course, one of the major factors in hot spot initiation. It is clear that crystal orientation has an important influence on localized temperature increase during the high rate of loadings. There are certain orientations, such as [100] for the uniaxial loading case, which are more amenable to plastic deformation and result in high local temperatures. However, other orientations such as [010] for the uniaxial loading case are rather brittle and do not have a significant contribution to the temperature increase.

A random texture or a texture contacting less deformable orientations leads to a lower temperature raise at the macroscale while a highly deformable texture shows significant plastic deformation which in turn results in a higher localized temperature rise. The temperature rises at microscale is much higher compared to those at macroscale which is related to the heterogeneity due to the presence of grains with different orientations at microstructural level.

These results have important implications in our understanding of the physics of hot spot initiation in heterogeneous explosives. Since hot spot initiation is a function of multiple variables (Bourne *et al.* 2003, Walley *et al.* 2006), it is important to consider damage of the crystals as a result of loading, which is left as future work. In this work, we have not studied the influence of unit cell size on the predicted response, which could be a valuable contribution if data regarding crystal orientation was available from experimentally determined pole figures.

## Acknowledgments

The authors gratefully acknowledge the support of this work through Office of Naval Research grants N000140510686 and N000140810462 with Dr. Clifford Bedford as the cognizant Program Manager.

## References

Abaqus (2009), ABAQUS Manual, Version 6.9, Simulia, Providence, RI.

- Baer, M.R. and Hall, C.A. (2007), "Isentropic loading experiments of a plastic bonded explosive and constituents", *J. Appl. Phys.*, **101**, 034906-034906-12.
- Barton, N.R., Winter, N.W. and Reaugh, J.E. (2009), "Defect evolution and pore collapse in crystalline energetic materials", *Modell. Simul. Mater. Sci. Eng.*, **17**, 035003.
- Becker, R. (2004), "Effects of crystal plasticity on materials loaded at high pressures and strain rates", *Int. J. Plasticity*, **20**, 1983-2006.
- Bourne, N.K. and Milne, A.M. (2003), "On cavity collapse and subsequent ignition", *Proc. 12th Int. Detonation Symp. (San Diego, CA)*, ed J.M. Short and D.G. Tasker, 213.
- Bowden, F.P. and Yoffe, A.D. (1952), *Initiation and growth of explosions in liquids and solids*, Cambridge, Cambridge University Press.
- Dick, J.J., Hooks, D.E., Menikoff, R. and Martinez, A.R. (2004), "Elastic-plastic wave profiles in cyclotetramethylene tetranitramine crystals", *J. Appl. Phys.*, **96**(1), 374-379.
- Hooks, D.E. and Ramos, K.J. (2006), "Initiation mechanisms in single crystal explosives: dislocations, elastic limits, and initiation thresholds", *Proc. 13th Int. Detonation Symp.*, Norfolk, VA.
- Kaczmarek, J. (2010), "Collection of dynamical systems with dimensional reduction as a multiscale method of modelling for mechanics of materials", *Interact. Multiscale Mech.*, **3**(1), 1-22.
- Macri, M. and De, S. (2006), "Modeling the bulk mechanical response of heterogeneous explosives based on microstructural information", *13th International Detonation Symposium*, Norfolk, VA.
- Mang, H.A., Aigner, E., Eberhardsteiner, J., Hackspiel, C., Hellmich, C., Hofstetter, K., Lackner, R., Pichler, B., Scheiner, S. and Stürzenbecher, R. (2009), "Computational multiscale analysis in civil engineering", *Interact. Multiscale Mech.*, **2**(2), 109-128.
- Matou, K. and Maniatty, A.M. (2009), "Multiscale modeling of elasto-viscoplastic polycrystals subjected to finite deformations", *Interact. Multiscale Mech.*, **2**(4), 375-396.
- Menikoff, R. and Sewell, T.D. (2002), "Constituent properties of HMX needed for meso-scale simulations", *Combust. Theor. Model.*, **6**, 103-125.
- Palmer, S.J.P. and Field, J.E. (1982), "The deformation and fracture of  $\beta$ -HMX", *Proc. Roy. Soc. Lond. A*, **383**, 399-407.
- Rae, P.J., Hooks, D.E. and Liu, C. (2006), "The stress versus strain response of single  $\beta$ -HMX crystals in quasi-static compression", *Proceedings of the 13th International Detonation Symposium*, Norfolk, VA.
- Sewell, T.D. and Menikoff, R. (2003), "A molecular dynamics simulation study of elastic properties of HMX", *J. Chem. Phys.*, **119**, 7417-7426.
- Taylor, G.I. (1938), "Plastic strain in metals", *J. Inst. Met.*, **62**, 307-324.
- Walley, S.M., Field, J.E. and Greenaway, M.W. (2006), "Crystal sensitivities of energetic materials", *Mater. Sci. Technol.*, **22**, 402-413.
- Wang, D. and Fang, L. (2010), "A multiscale method for analysis of heterogeneous thin slabs with irreducible three dimensional microstructures", *Interact. Multiscale Mech.*, **3**(3), 213-234.
- Yoo, C.S. and Cynn, H. (1999), "Equation of state, phase transition, decomposition of  $\beta$ -HMX", *J. Chem. Phys.*, **111**, 10229-10235.
- Zamiri, A.R., Pourboghra, F. (2010), "A novel yield function for single crystals based on combined constraints optimization", *Int. J. Plasticity*, **26**, 731-746.
- Zamiri, A.R. and De, S. (2010), "Deformation distribution map of  $\beta$ -HMX molecular crystals", *J. Phys. D: Appl. Phys.*, **43**, 035404.
- Zhang, X., Chen, J.S. and Osher, S. (2008), "A multiple level set method for modeling grain boundary evolution of polycrystalline materials", *Interact. Multiscale Mech.*, **1**(2), 178-191.